



Received: 15/01/2026

Revised: 13/02/2026

Accepted: 19/03/2026

Published online: 30/03/2026

Original Research Article



Open Access under the CC BY -NC-ND 4.0 license

UDC 536.8; 621.43; 662.613; 519.6

## COUPLED SPUTTERING AND COMBUSTION DYNAMICS OF DIVERSE FUEL TYPES

Bolegenova S., Askarova A., Ospanova Sh.<sup>\*</sup>, Bolegenova S.,  
Nurmukhanova A., Assilbekova Sh.

Department of Thermophysics and Technical Physics, Al-Farabi Kazakh National University, Almaty, Kazakhstan

\*Corresponding author: [Shynar.Ospanova@kaznu.edu.kz](mailto:Shynar.Ospanova@kaznu.edu.kz)

**Abstract.** *This study presents a comprehensive computational investigation of the sputtering and combustion dynamics of biodiesel and fossil diesel fuel droplets in turbulent gas flows. Advanced computational modeling and the CHEMKIN chemical kinetics framework were employed to analyze the thermophysical and chemical processes of fuel atomization, ignition, and flame propagation under varying oxidizer temperatures. The results indicate that biodiesel droplets exhibit higher mobility, enhanced mixing with the oxidizer, and more uniform heating, resulting in near-complete combustion and higher local temperatures compared to fossil diesel fuel. Soot formation during biodiesel combustion was notably lower, while carbon monoxide emissions were significantly reduced, demonstrating more efficient and cleaner combustion. Analysis of the Sauter mean diameter (SMD) highlighted improved droplet dispersion and atomization quality for biodiesel, facilitating optimized injector design and fuel-air mixing. Heat flux visualization revealed stronger convective energy transfer in biodiesel flames, and flame front dynamics confirmed that biodiesel can be used in conventional internal combustion engines without modification. Overall, these findings highlight biodiesel as a sustainable, low-emission alternative to fossil diesel fuel, supporting the development of energy-efficient technologies and the transition toward cleaner, renewable fuels.*

**Keywords:** Bioenergetics, Biodiesel, Fossil Fuel, Fuel Sputtering, Turbulent Combustion, Computational Modeling, Advanced Fuel Injection System, Pollutant Emissions

### 1. Introduction

Energy problems are growing every year and require both non-renewable natural energy resources and non-carbon forms of energy. Rising prices for traditional fuels and increasing environmental regulations necessitate a transition to alternative energy sources and the pursuit of biofuels derived from renewable resources. Alternative energy sources, in particular biofuels, have gained the status of a competitive energy source in both developed and developing countries. This was primarily due to the growing price competitiveness of technologies using renewable energy sources and biofuels, as well as political initiatives, the need to address energy and environmental security issues, the increasing demand for energy from developing and emerging economies worldwide, and the desire to make modern energy more accessible.

Global changes in the structure of energy production have led to the fact that today, the share of various types of biofuels in the total energy consumption, according to the World Bioenergy Association, is approximately 14% (. 1) [1]. The International Energy Agency (IEA) has set a target to use up to 80% of renewable energy sources by 2050 and halve CO<sub>2</sub> emissions as an indicator of the emission of harmful

substances [2-4]. As for Kazakhstan, several state laws and regulations on environmental protection have been developed that provide for the reduction of air pollution. In densely populated Kazakh cities with large traffic flows, the problem of gas pollution from the exhaust gases of internal combustion engines of vehicles is acute. According to the energy agency, more than 40% of pollutant emissions in Central Asia are generated by Kazakhstan [5, 6]. Biodiesel fuel is an alternative to fossil diesel fuel and can be used in diesel internal combustion engines (ICE), both in pure form and as a blend component. It has a slightly higher cetane number and better lubricity, which, when blended with traditional diesel fuel, ensures more stable engine operation. Biofuels contain virtually no sulfur and aromatic compounds, which significantly reduces the formation of harmful sulfur oxides and soot during their combustion.

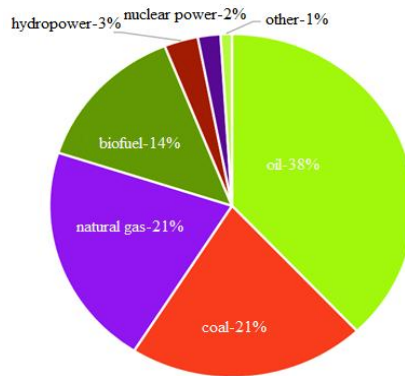


**Fig.1.** World energy consumption structure today

Most of the CO<sub>2</sub> generated during the combustion of biofuels is absorbed during the growth of plants used as raw materials, which ultimately reduces carbon dioxide emissions into the atmosphere by up to 80% compared to the use of fossil fuels [7, 8]. The technology for producing biodiesel fuel is theoretically simpler and less energy-consuming than the technology for producing traditional diesel fuel.

Problems related to global energy and environmental security require not only obtaining alternative energy sources but also the rational organization of their combustion. It is necessary to develop energy conversion systems that have higher efficiency and lower emissions of harmful substances. The efficiency of fuel consumption, productivity, and environmental friendliness of a power plant depend on the optimization of fuel combustion processes, which is associated with its preparation, method of supply, and proper combustion [9].

The above indicates the relevance of the identified problem and the need for a comprehensive study of heat and mass transfer processes during fuel combustion in energy devices. In this regard, this article is devoted to the use of the latest information technologies to study the combustion processes of liquid fuels (traditional fossil diesel fuel and biodiesel) in internal combustion engines.

In this work, for the first time, the processes of sputtering and combustion of biofuel droplets (biodiesel) were studied using information technologies and new 3D modeling software packages, to identify their advantages over fossil diesel fuel, with a subsequent assessment of the harmful emissions and greenhouse gases released during their combustion. The results of such research will contribute to the introduction of resource-saving energy technologies that meet modern environmental requirements.

## 2. Computational and spatial models of the problem

The mathematical model of the problem of atomization, combustion, and evaporation of liquid fuel droplets consists of equations of continuity, momentum, internal energy, and concentration of the reacting components of a two-phase flow [10-13]. The continuity equation of the fuel-air mixture is written as follows:

$$\frac{\partial \rho}{\partial t} + \operatorname{div}(\rho \mathbf{u}) = S_{\text{mass}}, \quad (1)$$

where  $\mathbf{u}$  is the fluid velocity,  $S_{\text{mass}}$  is the local change in gas density due to evaporation or condensation.

The mixture momentum equation has the form:

$$\rho \frac{\partial \mathbf{u}}{\partial t} + \rho (\text{gradu}) \mathbf{u} = \text{div} \boldsymbol{\xi} + \rho \mathbf{g} + \mathbf{S}_{\text{mom}}, \quad (2)$$

where  $\mathbf{S}_{\text{mom}}$  is the local rate of change in momentum of the gas phase due to the movement of droplets.

The conservation equation for internal energy has the following form:

$$\rho \frac{\partial E}{\partial t} = \boldsymbol{\tau} : \mathbf{D} - \rho \text{div} \mathbf{u} - \text{div} \mathbf{q} + \mathbf{S}_{\text{energy}}, \quad (3)$$

where  $\mathbf{q}$  is the specific heat flux expressed by Fourier's law, and  $\mathbf{S}_{\text{energy}}$  denotes the contribution to the change in internal energy due to the presence of the atomized liquid phase.

The conservation equation for the concentration of component  $m$  has the form:

$$\frac{\partial (\rho c_m)}{\partial t} = - \frac{\partial (\rho c_m u_i)}{\partial x_i} + \frac{\partial}{\partial x_i} \left( \rho D_{c_m} \frac{\partial c_m}{\partial x_i} \right) + \mathbf{S}_{\text{mass}}, \quad (4)$$

where  $\rho_m$  is the mass density of component  $m$ ,  $\rho$  is the total mass density.

For the numerical calculation of complex turbulent flows, we used the RANS method, which is widely used due to its simplicity, saving of computational resources, and a sufficient degree of accuracy in predicting the properties of reacting flows with chemical transformations. This method works well at high Reynolds numbers and high degrees of flow turbulence [14]. In our simulation, we used a prototype direct injection engine, where a jet of liquid fuel is sprayed at high pressure from multiple holes. In such internal combustion engines, fuel at a pressure of 200 bar is injected in the form of combinations of liquid ligaments and fragments of various sizes, which form near the injector nozzle and break into droplets, moving downstream due to interaction with air, which contributes to the growth of instability at the surface of the liquid. Figure 2 shows a schematic model of a multi-hole injector used in DI engines. The  $L_i/D_i$  ratio is a crucial parameter for this type of injector, as it influences the internal flow formation at the nozzle exit and the development of the spray structure [15, 16].

In an internal combustion engine with multi-hole injection, an individual injector is installed in the inlet pipe of each cylinder, supplying fuel directly to the intake valve, where the fuel mixture is prepared immediately before entering the combustion chamber. Therefore, the fuel-air mixture in multi-hole injection is uniform in composition and quality of flow for each of the cylinders, which has a beneficial effect on the power and efficiency of the engine, as well as on the toxicity of exhaust gases.

Figure 3 presents a perspective view of an unstructured computational grid composed of control volumes. This grid was generated using a set of specialized subroutines, allowing for the incorporation of various predefined initial parameters to accurately represent the computational domain.

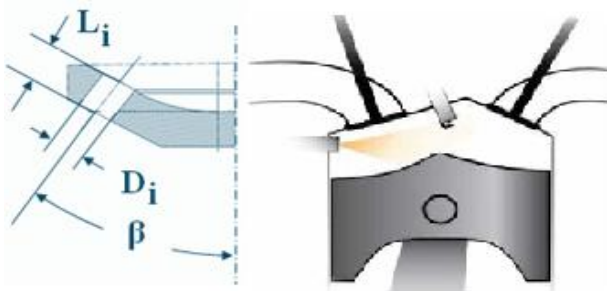


**Fig.2.** Schematic model of a direct injection:  
 $L_i$  –nozzle opening length;  $\beta$  – injection angle directed from the central axis of the injector;  $D_i$  – nozzle hole diameter.

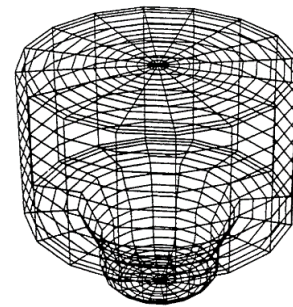


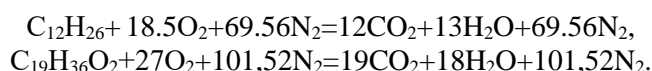
**Fig.3.** Perspective view of the used computational grid.

The highlighted region at the bottom of the grid, which contains several distinct subdomains, is filled with liquid fuel, providing the initial conditions necessary for simulating fuel injection, sputtering, and subsequent combustion processes. This visualization emphasizes the spatial distribution and connectivity of control volumes, which play a crucial role in capturing the detailed physical phenomena within the computational domain.

### 3. Computational modeling results and analysis

In this study, pure rapeseed biodiesel, specifically Biofuel RME B100, was employed as the biofuel. This fuel consists of a mixture of fatty acid methyl esters (FAME) derived from rapeseed oil. The predominant component is methyl oleate ( $C_{19}H_{36}O_2$ ), a monounsaturated ester, which constitutes approximately 90% of the total composition, accompanied by smaller amounts of saturated and polyunsaturated esters. The application of RME is particularly suitable under Kazakhstani conditions due to its enhanced cold-flow properties, which are crucial for the northern regions of the country. Furthermore, Kazakhstan's agroclimatic conditions are well-suited for rapeseed cultivation, rendering the production of RME both sustainable and economically viable on a national scale.

The equations for the complete combustion of fossil diesel fuel and biodiesel under internal combustion engine conditions with the participation of air are presented as follows:



In the engine, biodiesel undergoes combustion, producing carbon dioxide ( $CO_2$ ) and water ( $H_2O$ ), and releasing enough thermal energy to sustain engine operation. However, its energy content is slightly lower than that of conventional petroleum diesel fuel.

The chemical kinetics of biodiesel combustion, as well as its comparison with fossil diesel fuel, were simulated using the CHEMKIN code. This tool enables the development of detailed reaction mechanisms that comprehensively describe the thermodynamic and kinetic characteristics of fuel oxidation, including interactions between the fuel and the oxidizer [17]. The modeling framework incorporates critical parameters such as temperature, pressure, and flow velocity, providing a robust platform for accurately predicting the dynamics of combustion for both biodiesel and conventional diesel fuels. Importantly, this approach allows for the evaluation of pollutant formation while also assessing overall combustion efficiency. By integrating these factors, CHEMKIN facilitates a thorough understanding of the complex chemical and physical processes occurring during the combustion of different fuel types, offering valuable insights for optimizing engine performance and reducing harmful emissions.

In this study, computational experiments were conducted to investigate the sputtering and combustion dynamics of biofuel (biodiesel) droplets, as well as fossil petroleum diesel, in a turbulent gas flow. The effects of the initial oxidizer temperature on the sputtering, distribution, and combustion of both biodiesel and diesel fuel droplets within a model combustion chamber were systematically examined. This approach allowed for a detailed analysis of how temperature variations influence droplet dynamics, flame development, and the overall efficiency of the combustion process.

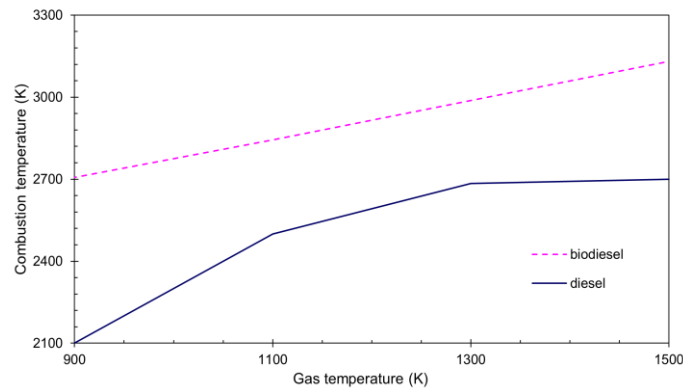
The dependence of the maximum fuel combustion temperature on the initial temperature of the oxidizer in the combustion chamber was determined for two types of liquid fuels. It has been established that combustion is not observed at an oxidizer temperature of less than 900 K. If the gas in the combustion chamber is heated to temperatures above 900 K, then in this case, there is combustion of liquid fuel with high heat release and heating of the chamber to 3000 K (Fig.4).

Figure 4 shows the dependence of the maximum fuel combustion temperature on the initial gas temperature. The maximum temperature during biodiesel combustion reaches about 3100 K, which is an indicator of combustion efficiency and the high heat capacity of biofuel. The initial gas temperature has the greatest influence on biodiesel combustion, as a 100 K increase in initial temperature results in a 1600 K increase in the maximum temperature in the combustion chamber.

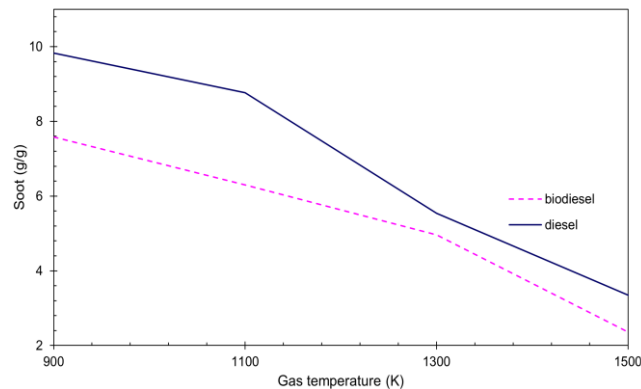
Since modern diesel engines are designed to reduce harmful emissions and be gentle on the environment, they have higher injection pressures than previous-generation diesel engines [18]. This means that the internal surfaces of engines are more likely to be subject to abrasion from soot and other contaminants.

Figure 5 shows the results of a comparative analysis of soot formation obtained using the global Shell model of chemical reactions [19]. The highest concentration of soot is formed during the combustion of petroleum diesel ( $9.8 \text{ g/m}^3$ ). When biodiesel burns, significantly less soot is released ( $7.5 \text{ g/m}^3$ ), which is a favorable reason for increasing engine efficiency and reducing fuel consumption and carbon dioxide emissions in the exhaust gases. The use of biodiesel as a fuel leads to a substantial reduction in carbon monoxide (CO) emissions compared to conventional petroleum diesel. While CO is inevitably formed during the combustion process, the amount released is considerably lower due to the higher oxygen content and more complete

combustion of biodiesel droplets. This improved combustion behavior limits the formation of incomplete combustion products, making biodiesel a cleaner alternative in terms of CO output. The reduction in CO emissions not only mitigates local air pollution but also contributes to lower health risks associated with carbon monoxide exposure.

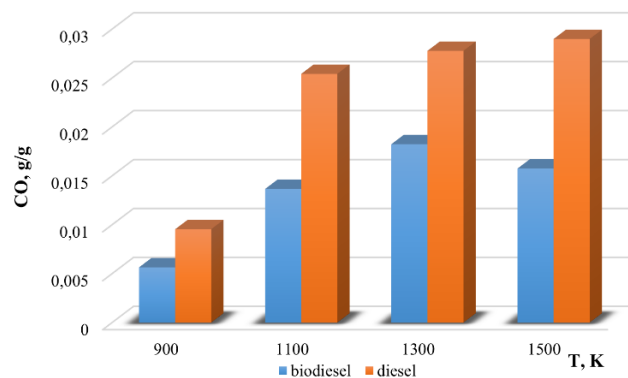


**Fig.4.** Temperature profiles during combustion of fossil diesel fuel and biodiesel depending on the initial gas temperature



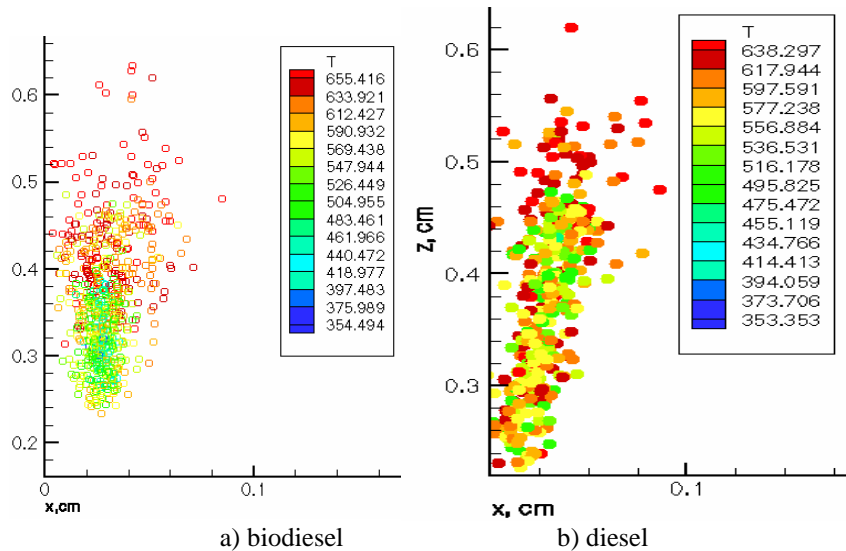
**Fig.5.** Soot formation during combustion of fossil diesel fuel and biodiesel depending on the initial gas temperature

The computational results indicate that, under the same operating conditions, engines fueled with biodiesel release significantly less CO than those running on traditional diesel, highlighting the environmental advantages of biodiesel in urban and industrial settings (Fig.6). Based on the analysis of the influence of gas temperature on the combustion processes and distribution of biodiesel and petroleum diesel droplets, a 3D visualization of the thermophysical characteristics of the reacting flow was obtained.



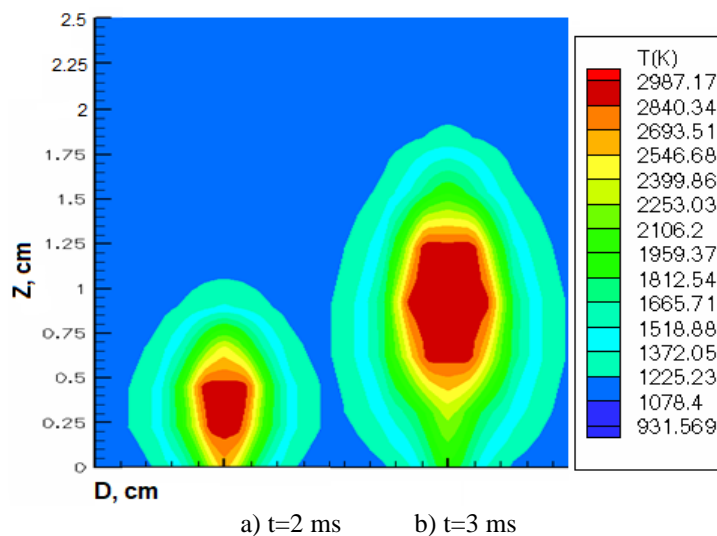
**Fig.6.** Carbon monoxide formation during combustion of biodiesel and diesel at different gas temperatures

Figure 7 shows graphs of droplet temperature distribution at 3 ms. The turbulent motion of the gas flow imparts additional kinetic energy to the droplets of both biodiesel and conventional diesel, accelerating them toward the exit of the combustion chamber. As a result of this rapid movement, the droplet temperature rises to over 600 K, promoting active chemical reactions.



**Fig.7.** Temperature distribution of diesel and biodiesel droplets along the height of the combustion chamber at  $t=3$  ms

Biodiesel droplets, in particular, exhibit higher mobility and respond more readily to the turbulent eddies within the chamber, leading to enhanced mixing with the surrounding oxidizer. This intensified interaction improves the local combustion environment, facilitates more uniform heating, and promotes near-complete combustion of the fuel droplets. Consequently, the dynamic behavior of biodiesel under turbulent conditions contributes to more efficient energy release and a reduction in unburned fuel residues, highlighting its advantages over conventional diesel in terms of combustion performance. In the case of combustion of a fuel-oxidizer premixed system, the temporal evolution of the biodiesel flame front is illustrated in Figure 8. The figure clearly demonstrates that both the shape and the size of the flame are strongly influenced by the degree of mixing between the fuel and the oxidizer. At 3 ms after ignition, the flame core extends from approximately 0.6 cm to 1.25 cm along the vertical axis of the combustion chamber. This elongation is attributed to elevated temperatures, which cause the boundary between the flame core and the ignition zone to expand, enhancing the propagation of the combustion front.



**Fig.8.** Variation of the biodiesel flame front over time

The flame morphology is inherently dependent on the properties of the flammable mixture and the characteristics of the injection system employed. Importantly, the combustion behavior of biodiesel indicates that it can be utilized in conventional internal combustion engine units without requiring modifications to the fuel delivery or injection system.

Beyond combustion performance, biodiesel exhibits a significant tribological benefit: its inherent lubricating properties reduce engine wear by approximately 60%, thereby extending the operational lifespan of critical engine components, including the fuel injection system, combustion chamber, and exhaust assembly. This combination of favorable flame dynamics and mechanical advantages underscores biodiesel's potential as a sustainable and efficient alternative to conventional petroleum diesel in automotive applications.

Figure 9 illustrates the distribution of heat flux in both biodiesel and diesel fuel mixtures reacting with an oxidizer. The visualization corresponds to the early stages of the ignition process, at a moment when the fuel has not yet fully reacted with the oxidizer. At this initial stage, the Nusselt number ranges between 1 and 2, reflecting the early development of convective heat transfer. Higher Nusselt numbers, in contrast, indicate regions of intense convective heat flux, which are characteristic of turbulent flow conditions.

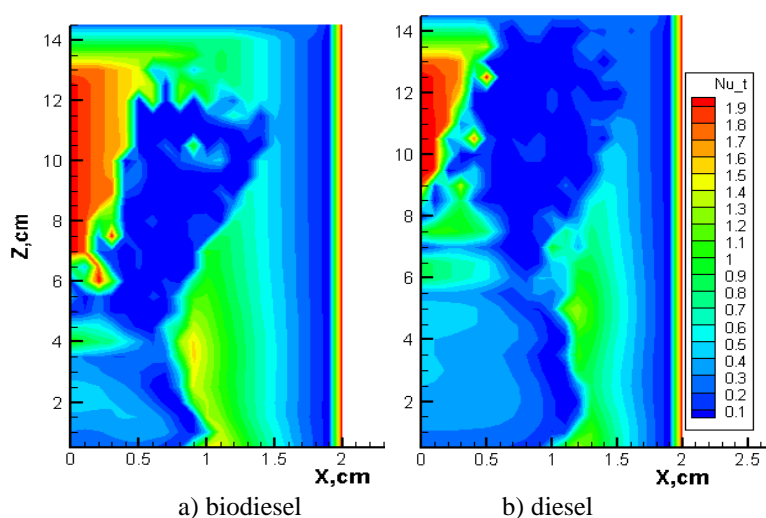


**Fig.9.** Visualization of heat flow intensity in a reacting mixture of biodiesel and oxidizer

As shown in Figure 9, the axis of the combustion chamber exhibits pronounced mixing of the fuel and oxidizer, driven by the temperature gradients within the flame core. For both biodiesel and diesel, this mixing plays a critical role in determining flame structure and combustion efficiency. However, due to differences in droplet mobility and fuel properties, biodiesel demonstrates more rapid and uniform mixing compared to conventional diesel, promoting earlier and more complete combustion. Additionally, the curvature of the flame front, previously observed in Figure 8, disrupts the formation of a flat, laminar combustion zone, leading to the development of a fully turbulent flame. This effect is more pronounced for biodiesel, where enhanced droplet dispersion and higher reactivity accelerate the transition from laminar to turbulent combustion, improving heat release rates and overall energy conversion.

Figure 10 illustrates the results of computational simulations tracking the temporal evolution of the Sauter mean diameter (SMD) of biodiesel droplets as a function of distance from the injector. These results are further compared with experimental data for conventional diesel fuel reported by [20], allowing for a direct evaluation of differences in atomization behavior between the two fuels. The Sauter mean diameter represents a key volumetric-surface parameter that characterizes the size distribution and atomization quality of liquid fuel droplets. Consequently, analysis of SMD provides critical information for the selection of injector design, optimization of fuel injection pressure, and determination of effective fuel flow rates necessary to achieve uniform droplet sizes throughout the combustion chamber. Such detailed characterization ensures improved fuel-air mixing and more efficient combustion, which is particularly important for enhancing engine performance and minimizing pollutant formation.

Analysis of Figure 10 indicates that the computational simulation results are generally in good agreement with the experimental data, with the exception of the region located approximately 10 mm from the injector

nozzle at 0.5 ms. In this zone, the calculated Sauter mean diameter (SMD) of biodiesel droplets reaches a peak value of 136  $\mu\text{m}$ , whereas the experimental measurements report a maximum SMD of 110  $\mu\text{m}$ .

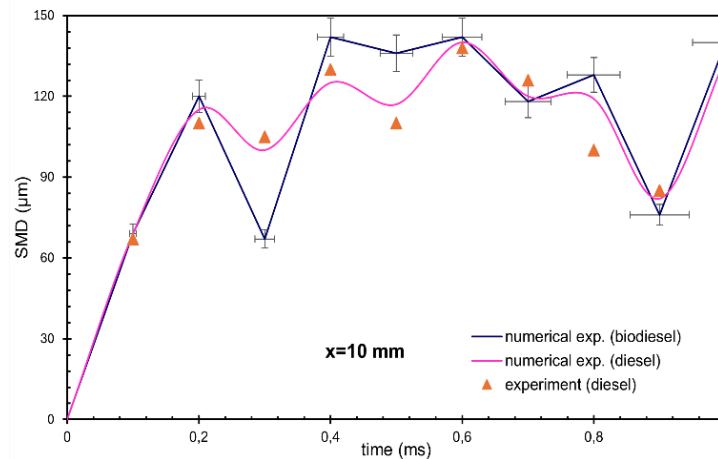


**Fig.10.** Comparison of time distributions of the Sauter mean diameter of droplets of diesel and biodiesel fuels at a distance of 10 mm from the injector nozzle

The observed discrepancies can be attributed to the proximity of the droplets to the injector, where end effects and localized flow disturbances are most pronounced. These phenomena inherently lead to deviations between the idealized conditions of numerical simulations and the complex dynamics captured in experimental observations, particularly in the near-nozzle region.

#### 4. Conclusions

From the results of the computational experiments of biodiesel and fossil diesel fuel droplets sputtering and combustion, the key findings regarding combustion efficiency, emissions, and droplet dynamics can be summarized as follows:

1. Biodiesel, specifically rapeseed methyl ester (RME B100), demonstrates significant potential as an alternative to conventional petroleum diesel. Its higher oxygen content, lower sulfur and aromatic compounds, and better lubricity contribute to more complete combustion, reduced emissions of soot and carbon monoxide (CO), and decreased engine wear. Computational results confirm that CO emissions from biodiesel are substantially lower than from fossil diesel fuel under identical operating conditions, highlighting its environmental and health advantages;

2. The combustion of biodiesel droplets in a turbulent gas flow shows enhanced mobility, improved mixing with the oxidizer, and more uniform heating compared to diesel droplets. This leads to near-complete combustion, higher local temperatures (up to  $\sim 3100$  K), and accelerated transition from laminar to turbulent flames. The shape and size of the flame front depend on fuel-oxidizer mixing and injection system characteristics, yet biodiesel can be utilized in standard diesel engines without modifications;

3. Visualization of heat flux indicates that biodiesel achieves more efficient convective heat transfer in the combustion chamber due to enhanced droplet dispersion and higher reactivity. Turbulent mixing promotes rapid flame propagation and effective energy release, contributing to higher combustion efficiency compared to fossil diesel fuel;

4. Analysis of the Sauter mean diameter (SMD) of fuel droplets shows that biodiesel exhibits slightly larger droplets near the injector due to end effects, but overall droplet dispersion and atomization are favorable. SMD analysis provides critical guidance for injector design, fuel injection pressure optimization, and uniform droplet formation, ensuring better fuel-air mixing and efficient combustion for both biodiesel and diesel;

5. The combined results of computational simulations and experimental comparisons indicate that biodiesel offers both environmental and operational advantages. Its use can reduce harmful emissions, improve engine lifespan due to natural lubrication, and provide a sustainable alternative in regions suitable for rapeseed cultivation, such as Kazakhstan. These findings support the broader adoption of biodiesel in internal combustion engines as part of a strategy to transition toward cleaner and renewable energy sources.

**Conflict of interest statement**

The authors declare that they have no conflict of interest in relation to this research, whether financial, personal, authorship or otherwise, that could affect the research and its results presented in this paper.

**CRedit author statement**

**Bolegenova S.:** Supervision; **Askarova A.:** Conceptualization, Funding acquisition; **Ospanova Sh.:** Investigation, Writing-Original draft preparation, Writing Reviewing and Editing; **Bolegenova S.:** Resources, Software; **Nurmukhanova A.:** Data curation, Methodology, Investigation; **Assilbekova S.:** Visualization, Validation.

The final manuscript was read and approved by all authors.

**Funding**

This work was supported by the Science Committee of the Science and Higher Education Ministry of the Republic of Kazakhstan (No 26105185).

**References**

1. The Global Bioenergy Statistics (GBS) report. WBA Global Bioenergy Statistics (2023). Available at: <https://www.worldbioenergy.org/news/763/47/WBA-publishes-the-Global-Bioenergy-Statistics-2023-report/>
2. AIKheder Sh., AIDousari A., AIOtaibi M. (2024) A simplified system dynamics model to investigate the effects of urban transportation management policies on reducing CO<sub>2</sub> and greenhouse gas emissions, *Phys. Chem. Earth.*, 135, 103623. <https://doi.org/10.1016/j.pce.2024.103623>
3. Pradhan R.P., Nair M.S., Hall J.H., Bennett S.E. (2024) Planetary health issues in the developing world: Dynamics between transportation systems, sustainable economic development, and CO<sub>2</sub> emissions, *J. Clean. Prod.*, 449, 140842. <https://doi.org/10.1016/j.jclepro.2024.140842>
4. Comineti C.S.S., Pretel A.F., Schlindwein M.M. (2023) The type of development promoted by Brazilian National Biofuels Policy, *Renew. Sustain. Energy Rev.*, 182, 113368. <https://doi.org/10.1016/j.rser.2023.113368>
5. Report of the IEA: IEA CO<sub>2</sub> Emissions from Fuel Combustion Statistics: Greenhouse Gas Emissions from Energy (2023). Available at: <https://www.iea.org/reports/co2-emissions-in-2023>
6. Askarova A., Bolegenova S., Ospanova S., Maxutkhanova A., Bolegenova K., Baidullayeva G. (2025) Study of thermophysical dynamics in biofuel droplet atomization and combustion, *Eurasian phys. tech. j.*, 22, 60–69. <https://doi.org/10.31489/2025N2/60-69>
7. Kiselev A., Magaril E., Karaeva A. (2024) Environmental and economic efficiency assessment of biogas energy projects in terms of greenhouse gas emissions, *Energ. Ecol. Environ.*, 9, 68–83. <https://doi.org/10.1007/s40974-023-00305-5>
8. EdwinGeo V., Fol G., Aloui F. et al (2021) Experimental analysis to reduce CO<sub>2</sub> and other emissions of CRDI CI engine using low viscous biofuels, *Fuel*, 283, 118829. <https://doi.org/10.1016/j.fuel.2020.118829>
9. Askarova A., Bolegenova S., Ospanova Sh., Slavinskaya N., Aldiyarova A., Ungarova N. (2021) Simulation of non-isothermal liquid sprays under large-scale turbulence, *Phys. Sci. Technol.*, 8, 28-40. <https://doi.org/10.26577/phst.2021.v8.i2.04>
10. Oruganti S.K., Gorokhovski M.A. (2024) Stochastic models in the under-resolved simulations of spray formation during high-speed liquid injection, *Phys. Fluids*, 36, 052105. <https://doi.org/10.1063/5.0206826>
11. Gorokhovski M.A., Oruganti S.K. (2022) Stochastic models for the droplet motion and evaporation in under-resolved turbulent flows at a large Reynolds number, *J. Fluid Mech.*, 932, 18. <https://doi.org/10.1017/jfm.2021.916>
12. Askarova A., Bolegenova S., Ospanova S., Bolegenova K., Nurmukhanova A. (2025) Energetic efficiency of turbulent biofuel combustion for advanced bioenergy technologies, *Int. J. Math. Phys.*, 16 (1), 20–28. <https://doi.org/10.26577/ijmph.20251612>
13. Zhong W., Xin Z., Wang L., Liu H. (2024) Investigations on High-Speed Flash Boiling Atomization of Fuel Based on Numerical Simulations, *Comput. Model. Eng. Sci.*, 139, 1427-1453. <https://doi.org/10.32604/cmescs.2023.031271>
14. Guo H., Li Y., Wang B., Zhang H., Xu H. (2019) Numerical investigation on flashing jet behaviors of single-hole GDI injector, *Int. J. Heat Mass Transf.*, 130, 50-59. <https://doi.org/10.1016/j.ijheatmasstransfer.2018.10.088>
15. Chang M., Kim H., Zhou B., Park S. (2023) Spray collapse resistance of GDI injectors with different hole structures under flash boiling conditions, *Energy*, 268, 126689. <https://doi.org/10.1016/j.energy.2023.126689>
16. Geissler C.H., Ryu J., Maravelias Ch.T. (2024) The future of biofuels in the United States transportation sector, *Renew. Sustain. Energy Rev.*, 192, 114276. <https://doi.org/10.1016/j.rser.2023.114276>
17. Ra Y., Reitz R.D. (2008) A reduced chemical kinetic model for IC engine combustion simulations with primary reference fuels, *Combust. Flame*, 155, 713–738. <https://doi.org/10.1016/j.combustflame.2008.05.002>
18. Yin Z., Liu S., Tan D., Zhang Z., Wang Z., Wang B. (2023) A review of the development and application of soot modelling for modern diesel engines and the soot modelling for different fuels, *Process. Saf. Environ. Prot.*, 178, 836-859. <https://doi.org/10.1016/j.psep.2023.08.075>

19. Cui M., Zhang W., Fu J., Luo X., Hung D.L.S., Xu M., Li X. (2024) Impact of flash boiling spray on soot generation of a rich fuel–air mixture under various ambient pressures, *Combust. Flame*, 263, 113388. <https://doi.org/10.1016/j.combustflame.2024.113388>
20. Arcoumanis C, Gavaises M, French B (1997) Effect of fuel injection processes on the structure of diesel sprays. *SAE Technical Paper*, 970799. <https://doi.org/10.4271/970799>

---

#### AUTHORS' INFORMATION

**Bolegenova, Saltanat Alikhanovna** – Doctor of Phys. and Math. Sciences, Professor, Head of the Department of Thermophysics and Technical Physics, Al-Farabi Kazakh National University, Almaty, Kazakhstan; SCOPUS Author ID: 57192917040; <https://orcid.org/0000-0001-5001-7773>; [Saltanat.Bolegenova@kaznu.edu.kz](mailto:Saltanat.Bolegenova@kaznu.edu.kz)

**Askarova, Aliya Sandybayevna** – Doctor of Phys. and Math. Sciences, Professor, Department of Thermophysics and Technical Physics, Al-Farabi Kazakh National University, Almaty, Kazakhstan; SCOPUS Author ID: 6603209318; ORCID: <https://orcid.org/0000-0003-1797-1463>; [Aliya.Askarova@kaznu.edu.kz](mailto:Aliya.Askarova@kaznu.edu.kz)

**Ospanova, Shynar Sabitovna** – PhD, Senior Lecturer, Department of Thermophysics and Technical Physics, Al-Farabi Kazakh National University, Almaty, Kazakhstan; Scopus Author ID: 55988678700; ORCID ID: 0000-0001-6902-7154; [Shynar.Ospanova@kaznu.edu.kz](mailto:Shynar.Ospanova@kaznu.edu.kz)

**Bolegenova, Symbat Alikhanovna** – PhD, Associate Professor, Department of Thermophysics and Technical Physics, Al-Farabi Kazakh National University, Almaty, Kazakhstan, Scopus Author ID: 57195694754; ORCID: 0000-0003-1061-6733; [Bolegenova.Symbat@kaznu.edu.kz](mailto:Bolegenova.Symbat@kaznu.edu.kz)

**Nurmukhanova, Alfiya Zeinullova** – Candidate of Tech. Sciences, Department of Thermophysics and Technical Physics, Al-Farabi Kazakh National University, Almaty, Kazakhstan, Scopus Author ID: 57217224044; ORCID: 0000-0002-0289-3610; [alfiyanurmukhanova7@gmail.com](mailto:alfiyanurmukhanova7@gmail.com)

**Assilbekova, Shira Kultubayevna** – PhD student, Department of Thermophysics and Technical Physics, Al-Farabi Kazakh National University, Almaty, Kazakhstan, ORCID: 0009-0000-2246-1033; [Asilbekovashira6@gmail.com](mailto:Asilbekovashira6@gmail.com)